Available online at www.sciencedirect.com
ScienceDirect
Journal of Sound and Vibration 312 (2008) 273–295
JOURNAL OF SOUND AND VIBRATION
www.elsevier.com/locate/jsvi

Nonlinear dual-axis biodynamic response of the semi-supine human body during longitudinal horizontal whole-body vibration

Ya Huang, Michael J. Griffin*

Human Factors Research Unit, Institute of Sound and Vibration Research, University of Southampton, Southampton SO17 1BJ, UK

Received 15 February 2007; received in revised form 18 October 2007; accepted 23 October 2007
Available online 18 December 2007

Abstract

The resonance frequencies in frequency response functions of the human body (e.g. apparent mass and transmissibility) decrease with increasing vibration magnitude. This nonlinear biodynamic response is found with various sitting and standing postures requiring postural control. The present study measured the apparent mass of the body in a relaxed semi-supine posture with two types of longitudinal horizontal vibration (in the z-axis of the semi-supine body): (i) continuous random excitation (0.25–20 Hz) at five magnitudes (0.125, 0.25, 0.5, 0.75 and 1.0 ms^{-2} rms); (ii) intermittent random excitation (0.25–20 Hz) alternately at 0.25 and 1.0 ms^{-2} rms. With continuous random vibration, the dominant primary resonance frequency in the median normalised apparent mass decreased from 3.7 to 2.4 Hz as the vibration magnitude increased from 0.125 to 1.0 ms^{-2} rms. A nonlinear response was apparent in both the horizontal (z-axis) apparent mass and the vertical (x-axis) cross-axis apparent mass. With intermittent random vibration, as the vibration magnitude increased from 0.25 to 1.0 ms^{-2} rms, the median resonance frequency of the apparent mass decreased from 3.2 to 2.5 Hz whereas, with continuous random vibration over the same range of magnitudes, the resonance frequency decreased from 3.4 to 2.4 Hz. The median change in the resonance frequency (between 0.25 and 1.0 ms^{-2} rms) was 0.6 Hz with the intermittent random vibration and 0.9 Hz with the continuous random vibration. With intermittent vibration, the resonance frequency was higher at the high magnitude and lower at the low magnitude than with continuous vibration at the same magnitudes. The responses were consistent with passive thixotropy being a primary cause of nonlinear biodynamic responses to whole-body vibration, although reflex activity of the muscles may also have an influence.

1. Introduction

The resonance frequencies in frequency response functions of the human body (e.g. apparent mass and transmissibility) decrease with increasing vibration magnitude—the median apparent mass resonance frequencies of a group of 12 seated human subjects were, respectively, 5.4, 5.0, 4.7, 4.6, 4.4 and 4.2 Hz with vibration magnitudes of 0.25, 0.5, 1.0, 2.0 and 2.5 ms^{-2} rms [1]. This nonlinear biodynamic response has been found in studies of apparent mass and transmissibility with various sitting postures (e.g. Refs. [2–4]) and

*Corresponding author. Tel.: +44 23 8059 2277; fax: +44 23 8059 2927.
E-mail address: M.J.Griffin@soton.ac.uk (M.J. Griffin).

0022-460X/$ - see front matter © 2007 Elsevier Ltd. All rights reserved.
doi:10.1016/j.jsv.2007.10.047

standing postures [5,6] that require muscular postural control. The nonlinearity is evident in both the vertical and the fore-and-aft responses of the seated human body during vertical whole-body vibration [3], and in both the fore-and-aft and vertical responses of the seated human body during fore-and-aft whole-body vibration [4,7].

Electromyographic (EMG) studies indicate that the activity of the back muscles varies with vibration magnitude [8,9]. So muscular activity could be a cause of the nonlinearity: muscles may stabilise or stiffen the body at low magnitudes of vibration but be incapable of a sufficient response at high magnitudes where there are greater inertial forces. With 12 subjects sitting upright without a backrest, Huang and Griffin [10] found the nonlinearity could be significantly reduced by some voluntary periodic upper-body movements. The apparent mass resonance frequencies were 5.5 Hz at 0.25 ms^{-2} rms and 4.4 Hz at 2.0 ms^{-2} rms without voluntary movements, but 4.7 Hz at 0.25 ms^{-2} rms and 4.6 Hz at 2.0 ms^{-2} rms with voluntary movements. The change in nonlinearity due to voluntary movement was considered to be due to either a change in muscular activity stimulated by the voluntary periodic contraction or a change in the stiffness of the body due to the thixotropic behaviour of body tissues.

'Thixotropy' refers to a recovery behaviour of colloidal materials after the breakdown of structural linkages [11]. Perturbations break down the structures but after a period of stillness the structures reform. Some human body tissues (protoplasm, mucus, etc.) have a similar thixotropic behaviour [12]. Lakie [13] found a thixotropic response in human index fingers in response to tap stimuli—the dynamic stiffness of the finger increased back to normal about 10 s after an impulse. The nonlinearity in the human body during whole-body vibration could be a consequence of thixotropy: the equivalent stiffness of the body decreasing during high-magnitude vibration and the stiffness increasing after vibration or with low magnitudes of vibration.

Huang and Griffin [14] compared the apparent mass of the semi-supine body measured with intermittent vertical vibration and continuous vertical vibration. The intermittent vibration (alternately 1.0 and 0.25 ms^{-2} rms) allowed the apparent mass to be measured 2.56 s after the commencement of high-magnitude or the low-magnitude vibration. With continuous random vibration, the apparent mass resonance frequencies were 9.6 and 7.8 Hz with magnitudes of 0.25 and 1.0 ms^{-2} rms, respectively. Whereas with intermittent vibration, the resonance frequencies were 9.3 and 8.1 Hz at 0.25 and 1.0 ms^{-2} rms, respectively. The responses with intermittent vibration were consistent with the resonance frequency, or the dynamic stiffness, of the body depending on the shear history of the body, typical of thixotropy. However, the changes could be caused by either muscle activity (involuntary or voluntary) or a passive change in the body tissues. In a relaxed semi-supine posture there is little muscle activity compared to sitting and standing postures, so the nonlinear response may be more likely due to thixotropic changes than muscular contractions. If thixotropy is the primary cause of the nonlinearity in the in-line and cross-axis responses with various directions of excitation, the dependence on the shear history found with vertical excitation of the semi-supine body should also be present with longitudinal horizontal excitation.

As part of a series of studies to explore the biodynamic nonlinearity [10,14], the present study investigated the longitudinal in-line and the cross-axis vertical biodynamic responses of the relaxed semi-supine body exposed to longitudinal horizontal whole-body vibration. It was designed to find out whether the response of the body is nonlinear with both continuous and intermittent random vibration, and if the intermittency (changed shear history) has an effect on the nonlinearity.

It was hypothesised that, with continuous random whole-body vibration, the longitudinal in-line apparent mass resonance frequencies and vertical cross-axis apparent mass peak frequencies would decrease with increasing vibration magnitude. It was also hypothesised that with intermittency the in-line resonance frequencies and the cross-axis peak frequencies would be decreased by prior high-magnitude vibration and increased by prior low-magnitude vibration compared to the resonance frequencies and peak frequencies measured at the same high and low magnitudes of continuous vibration.

2. Method

2.1. Apparatus

A supine support was constructed with three parts: back support, leg rest and headrest (Fig. 1). The experimental set-up was the same as used in the preceding study with vertical vibration [14] to allow the same semi-supine postures to be tested.

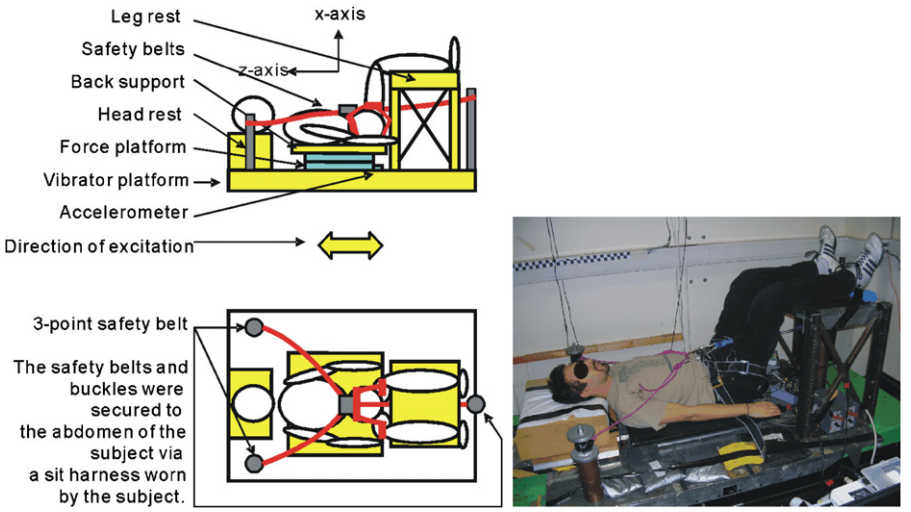

Fig. 1. Schematic diagram of the supine support showing the semi-supine posture and the axes of the forces (z-axis and x-axis) and the acceleration (z-axis) transducers. A photographic representation of a test subject in the relaxed semi-supine position for longitudinal horizontal (z-axis) whole-body vibration.

The back support was a horizontal flat rigid 660 mm × 660 mm × 10 mm aluminium plate with a high stiffness 3 mm thick laterally treaded rubber layer attached to the upper surface. The complete back support was bolted rigidly to the upper surface of the force platform, which monitored the longitudinal forces (in the z-axis of the semi-supine subject) and the vertical forces (in the x-axis of the semi-supine subject) exerted by the subject on the back support. The force platform was bolted rigidly to the vibrator platform. The horizontal distance between the edge of the back support and the edge of the leg rest was 50 mm (Fig. 1).

The legs of subjects rested on a horizontal flat rigid aluminium support with an 8-mm thick high stiffness rubber layer attached to the top. The height of the leg rest was adjusted to allow the lower legs to rest horizontally.

The headrest was a horizontal flat rigid wooden block with 75-mm thick car-seat foam attached to the upper surface. The top surface of the complete headrest was approximately 50 mm higher than the back support. The horizontal distance between the back support and the headrest was adjusted by moving the headrest so that a subject's head could rest comfortably.

Longitudinal horizontal vibration (in the z-axis of the subjects) was produced by a 1-m stroke electro-hydraulic horizontal vibrator capable of accelerations up to $\pm 10\,\mathrm{ms}^{-2}$ in the laboratory of the Human Factors Research Unit.

The longitudinal horizontal (z-axis) acceleration of the vibrator platform was measured using a Setra 141A ± 2 g accelerometer fixed on the plane of vibrator platform below the back support and between the leg rest and the force platform (Fig. 1). The longitudinal horizontal (z-axis) and the vertical (x-axis) forces at the back support were measured using a Kistler 9281 B21 12-channel force platform. The four longitudinal horizontal (z-axis) force signals and the four vertical (x-axis) force signals from the four corners of the platform were summed and conditioned using two Kistler 5001 charge amplifiers.

An *HVLab* v3.81 data acquisition and analysis system was used to generate test stimuli and acquire the longitudinal acceleration and the longitudinal and vertical forces from the transducers. The one acceleration and the two force signals were acquired at 200 samples per second via 67 Hz analogue anti-aliasing filters.

2.2. Stimuli

The random stimuli used in this study had approximately flat constant-bandwidth acceleration power spectra over the frequency range 0.25–20 Hz.

Two types of longitudinal horizontal vibration were employed:

(i) Continuous random vibration with a duration of 90 s tapered at the start and end with 0.5-s cosine tapers. Five magnitudes of acceleration (0.125, 0.25, 0.5, 0.75 and 1.0 ms^{-2} rms, unweighted) were generated using five different random seeds. Twelve subjects were randomly divided into six groups with two persons per group. With different groups, different random seeds were used to generate the random stimuli.

(ii) Intermittent random vibration, alternately at 0.25 and 1.0 ms^{-2} rms (unweighted) with a total duration of 828 s. The 828-s intermittent stimulus was divided evenly into four identical 207-s sections (Fig. 2a). During each 207-s section, 18 high-magnitude slices and 18 low-magnitude slices (generated using different random seeds) were presented alternately. The duration of 828 s was determined so that there were sufficient high-magnitude and low-magnitude slices for the concatenated signals (at high or low magnitude) to have the same duration as each of the continuous signals (i.e., 90 s). One single cycle of the intermittent signal was defined as one high-magnitude slice followed by one low-magnitude slice. During a single cycle of the intermittent motion, the high-magnitude slice (at 1.0 ms^{-2} rms) lasted for 6 s (tapered at the start and end with a 0.25-s cosine taper) followed by a low-magnitude slice (at 0.25 ms^{-2} rms) for 5.5 s (Fig. 2b). The durations of the high or low-magnitude slices were determined so that the effective high or low-magnitude signals (after removing the tapering) could be analysed with a frequency resolution of about 0.4 Hz (see Section 2.5.2).

All test motions were presented in one session lasting approximately 100 min. The order of presentation of the six random stimuli (the continuous stimuli at five magnitudes and the intermittent stimulus) was balanced across the twelve subjects.

2.3. Posture

While experiencing each motion, subjects maintained a relaxed semi-supine position with their lower legs lifted and resting on the horizontal leg rest so as to give maximum back contact with the back support (Fig. 1). The longitudinal horizontal distance between the bottom of the buttocks (aligned with the edge of the back support) and the near edge of the leg rest was 50 mm for all subjects. Subjects were instructed to relax totally with their eyes closed. The semi-supine posture was the same as described by Huang and Griffin [14].

For safety, subjects wore a light harness connected by three loose safety belts to the vibrator platform without constraining the movement of the body. The total weight of the harness and buckles was less than 0.5 kg.

2.4. Subjects

Twelve male subjects, aged between 20 and 42 years, with median (minimum and maximum) stature 1.73 m (1.66 and 1.80 m) and median total body mass 66.4 kg (58.3 and 86.2 kg) participated in the study. The study used the same subjects and the same testing order as the preceding study with vertical excitation [14].

The experiment was approved by the Human Experimentation, Safety and Ethics Committee of the Institute of Sound and Vibration Research at the University of Southampton.

2.5. Analysis

The analysis was similar to that used with vertical excitation [14]. The data were analysed over the frequency 0.25–20 Hz, but the presentation of results is limited to 0.5–10 Hz. The magnitude of the horizontal apparent mass at frequencies greater than 10 Hz was small (about 5–15% of the static body mass and 2–6% of the apparent mass at resonance).

2.5.1. Continuous random vibration

The longitudinal horizontal (z-axis) and vertical (x-axis) forces measured at the supine back support were analysed relative to the longitudinal horizontal (z-axis) acceleration (Fig. 1). Two frequency response functions—longitudinal apparent mass (where the force was in-line with the acceleration in the longitudinal

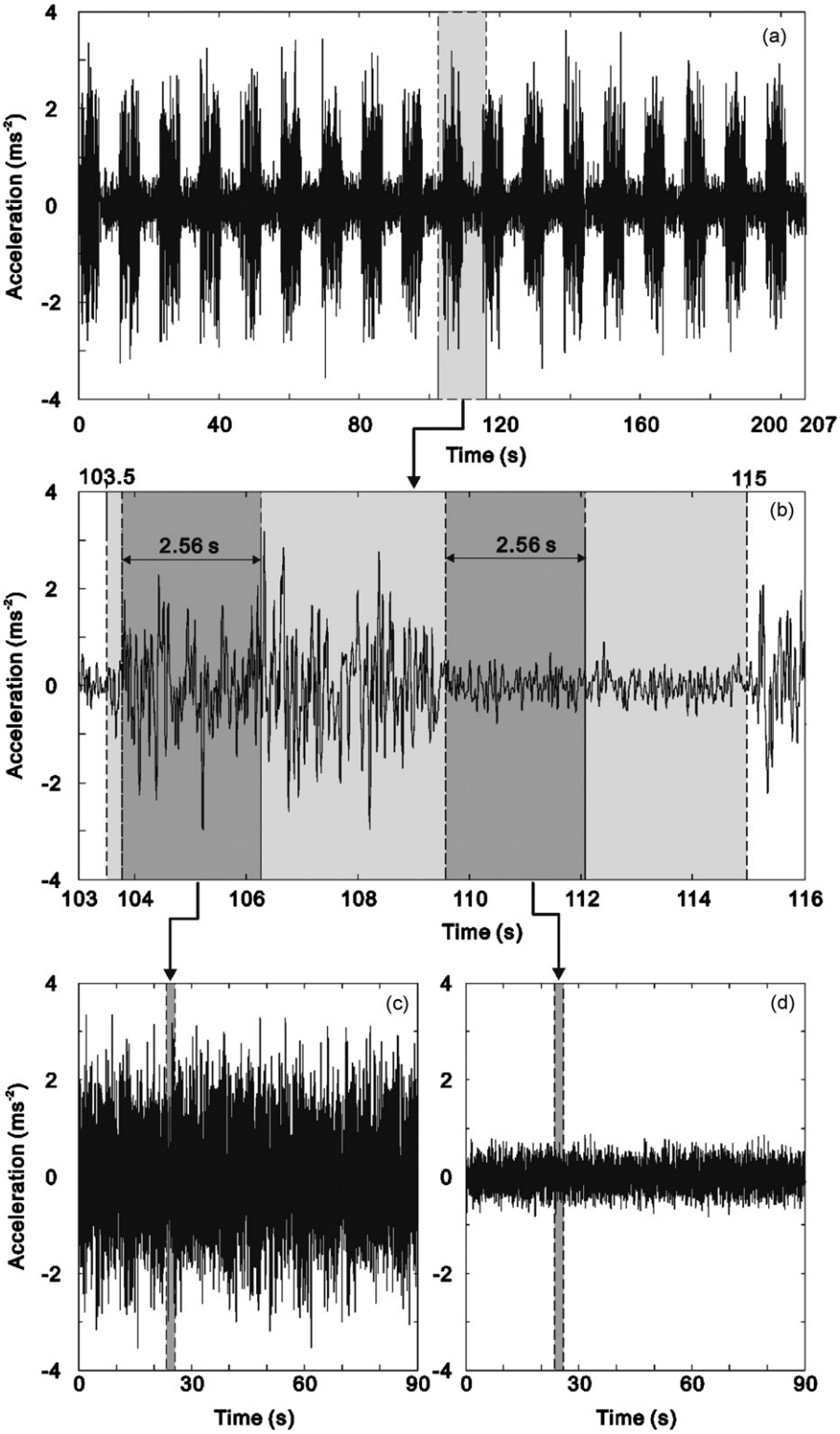

Fig. 2. An example of a longitudinal excitation acceleration time history measured with the high–low (1.0–0.25 s^{-2} rms) magnitude intermittent random stimuli showing: (a) one complete 207-s intermittent time history; (b) one period of the intermittent time history starting with 6-s high-magnitude slice followed by a 5.5-s low-magnitude slice; (c) extracted and concatenated high-magnitude (1.0 ms^{-2} rms) time slices (2.56 s each); (d) extracted and concatenated low-magnitude (0.25 ms^{-2} rms) time slices (2.56 s each). The same procedure was applied to longitudinal force and vertical cross-axis force time histories.

horizontal direction, i.e. the z-axis) and vertical cross-axis apparent mass (where the vertical force was perpendicular to the longitudinal acceleration in the sagittal plane, i.e. the x-axis)—were calculated using the cross-spectral density method (CSD):

$$M(f) = S_{af}(f)/S_{aa}(f), \tag{1}$$

where $M(f)$ is the longitudinal apparent mass or the vertical x-axis cross-axis apparent mass, in kg; $S_{af}(f)$ is the CSD between the measured forces and the longitudinal excitation acceleration; and $S_{aa}(f)$ is the power spectral density (PSD) of the longitudinal excitation acceleration.

Before calculating the longitudinal apparent mass, mass cancellation was carried out in the time domain to subtract the force caused by the masses above the force sensing elements (a total of 30.5 kg obtained dynamically in the frequency range 0.25–20 Hz). No mass cancellation was needed to calculate the vertical cross-axis apparent mass as there was no input motion in this direction.

The relation of the output motion to the input motion in the calculated frequency response functions was investigated using the coherency:

$$\gamma^2_{io}(f) = |S_{af}(f)|^2/(S_{aa}(f)S_{ff}(f)), \tag{2}$$

where $S_{ff}(f)$ is the PSD of the longitudinal force and $\gamma^2_{io}(f)$ is the coherency of the system with a value between 0 and 1. The coherency has a maximum value of 1.0 in a linear single-input system with no noise—the output motion being entirely due to, and linearly correlated with, the input motion.

The apparent masses at the five magnitudes were normalised by dividing by the apparent mass modulus measured at frequencies between 0.25 and 1.5 Hz, where the body was considered rigid. For motion at 0.125 ms^{-2} rms, the normalisation was carried out at 0.98 Hz; for 0.25 ms^{-2} rms at 0.98 Hz; for 0.5 ms^{-2} rms at 0.59 Hz; for 0.75 ms^{-2} rms at 0.59 Hz; for 1.0 ms^{-2} rms at 0.39 Hz. The median normalised apparent masses at the five magnitudes were then calculated. The same normalisation procedure was applied to calculate the normalised vertical cross-axis apparent mass at the five magnitudes. The median normalised x-axis cross-axis apparent masses were then calculated.

The CSD and PSD were estimated via Welch's method at frequencies between 0.25 and 20 Hz (data shown 0.25–10 Hz). The frequency response functions for each of the 90-s continuous random signals used a fast Fourier transform (FFT) windowing length of 2048 samples, a hamming window with 100% overlap, a sampling rate of 200 samples per second and an ensuing frequency resolution of 0.1 Hz (see Table 1). This signal processing procedure applied to signals measured with continuous vibration is referred as the 0.1-Hz procedure.

2.5.2. Intermittent random vibration

Before the intermittent signals (longitudinal acceleration, longitudinal force and vertical force) were analysed according to the procedure applied to the continuous signals (Section 2.5.1), the acquired intermittent signals described in Section 2.2(ii) were processed as described below.

Each of the high-magnitude (1.0 ms^{-2} rms) and low-magnitude (0.25 ms^{-2} rms) time slices of the acceleration and forces measured with each of the 828-s intermittent signals was extracted and concatenated into a processed high-magnitude signal (90 s duration) and a processed low-magnitude signal (90 s duration) (Fig. 2c, d). The duration of each extracted time slice was 2.56 s to allow the apparent masses to be measured and calculated before the dynamic stiffness of the body recovered from the prior high-magnitude or low-magnitude vibration. Each of the force and acceleration time histories measured with the continuous random stimuli and each of the processed force and acceleration time histories measured with the intermittent random stimuli lasted for 90 s, allowing the apparent masses to be calculated with the same frequency resolution of 0.4 Hz for both stimuli. The 0.4-Hz procedure used 0% overlap; any discontinuity caused by the concatenation of the 2.56-s slices had an effect at frequencies lower than of interest in the present study (Table 1).

The same procedure used to analyse the signals measured with continuous random vibration (Section 2.2(i)) was used to calculate the apparent masses and cross-axis apparent masses with each of the 90-s high-magnitude (1.0 ms^{-2} rms) and low-magnitude (0.25 ms^{-2} rms) processed intermittent signals, except for a different signal processing procedure (0.4-Hz procedure, Table 1). The 0.4-Hz procedure was used to generate apparent masses and cross-axis apparent masses with each of the 90-s processed intermittent acceleration and

Table 1
Two signal processing procedures used to analyse measurement with the continuous random vibration and with the intermittent random vibration

Duration (s)	Sampling rate (Hz)	FFT length	Degrees of freedom	Windowing overlap (%)	Frequency resolution (Hz)
(A) 0.1-Hz procedure—for measured accelerations and forces with continuous random vibration at 0.125, 0.25, 0.5, 0.75 and 1.0 ms^{-2} rms					
90	200	2048	36	100	0.10
(B) 0.4-Hz procedure—for processed accelerations and forces measured at 0.25 and 1.0 ms^{-2} rms for both the intermittent and continuous random vibration					
90	200	512	70	0	0.40 (then linearly interpolated to 0.10 in the frequency domain)

force signals. The 0.4-Hz procedure was also used to analyse accelerations and forces measured with the continuous vibration at 0.25 and 1.0 ms^{-2} rms so that the apparent masses measured with the intermittent and the continuous vibration could be compared using the same frequency resolution (0.4 Hz) with the same signal duration (90 s). Finally, the frequency resolution obtained using the 0.4-Hz procedure with both intermittent and continuous signals at 0.25 and 1.0 ms^{-2} rms was increased to 0.1 Hz by linearly interpolating the apparent mass moduli and phases in the frequency domain.

2.5.3. Curve fitting, apparent mass resonance frequencies and cross-axis apparent mass peak frequencies

The parallel two-degree-of-freedom parametric model used to fit the vertical in-line individual apparent masses and phases [10,14] was adapted to fit the longitudinal in-line individual apparent masses and phases in order to obtain primary resonance frequencies. The two vertical (x-axis) degrees of freedom in the model were transformed into two longitudinal (z-axis) horizontal degrees of freedom, and the direction of the input excitation was changed from vertical to longitudinal in the horizontal plane (Fig. 6). The lumped parameter model was employed as a numerical tool to characterise the apparent mass of the human body. It was not a mechanistic model representing any physical mechanisms or anatomical parts of the body in response to whole-body vibration.

To quantify the biodynamic nonlinearity, the primary resonance frequencies of both the individual and the median normalised apparent masses are represented by the frequency at which the modulus of the apparent mass was a maximum in the fitted curve. Model parameters also allowed the dynamic characteristics of the body to be quantified over the full fitting frequency range interested.

The vertical x-axis cross-axis apparent mass 'peak frequency' was defined as the frequency at which the modulus of the measured cross-axis apparent mass had a maximum value in the frequency range 0.5–10 Hz. In this frequency range, there were one, two or three peaks depending on the vibration magnitude and inter-subject variability. The first dominant peak below about 5 Hz was used to represent the dynamic characteristic of the vertical cross-axis response of the body (Section 3.2.1).

The curve-fitting method used a constrained minimum error search command 'fmincon()' of the optimisation toolbox of *MATLAB* (version 7.0.1, R14, SP1). The target error was calculated by summing the square of the errors in the modulus (kg) and the phase (rad) at each frequency point between the measurement and the fitted curve. Before summation, the modulus errors were re-scaled to have an equivalent scale to the phase errors by multiplying the modulus (at each frequency point from 0.5 to 10 Hz) by a normalisation factor P:

$$P = |\mathrm{PH}_s|_{\max}/|\mathrm{AM}_s|_{\max}, \tag{3}$$

where $|\mathrm{AM}_s|_{\max}$ is the maximum value of the modulus of the measured apparent mass (kg) at any frequency point between 0.5 and 10 Hz, and $|\mathrm{PH}_s|_{\max}$ is the maximum absolute value of measured phase (rad). Therefore, the normalisation was based on the values at two frequencies: one giving the maximum modulus and the other giving the maximum absolute phase.

The apparent mass modulus errors were then summed over the frequency range 0.5–10 Hz. The phase errors were calculated similarly except that they were not normalised (by the factor P) but multiplied by an empirical

phase weighting factor Q (given a value of 5.0) in order to produce the best fit (using the same model [15] found better fitting results with higher weightings on phase). The overall target error (cost function) was expressed of the form:

$$E = \sum_{N_f}\{P[\mathrm{AM}_m(f) - \mathrm{AM}_s(f)]^2\} + \sum_{N_f}\{Q[\mathrm{PH}_m(f) - \mathrm{PH}_s(f)]^2\}, \quad (4)$$

where E is the overall target error between the fitted curve and measured apparent masses; N_f is the number of frequency points in the measured apparent mass; $\mathrm{AM}_m(f)$ and $\mathrm{PH}_m(f)$ are the apparent mass modulus and phase of the model at each frequency; $\mathrm{AM}_s(f)$ and $\mathrm{PH}_s(f)$ are the measured apparent mass modulus and phases at each frequency; P is the normalisation factor for apparent mass modulus, Eq. (4); $Q = 5.0$ is the phase weighting factor; and f refers to the frequencies of curve-fitting from 0.5 to 10 Hz.

The same curve-fitting procedure was carried out with the longitudinal apparent masses at the five magnitudes (0.125, 0.25, 0.5, 0.75 and 1.0 ms^{-2} rms) of continuous random vibration and the two magnitudes (0.25 and 1.0 ms^{-2} rms) of processed intermittent random vibration.

By fitting the parallel two-degree-of-freedom model to the longitudinal apparent mass, the apparent mass resonance frequency (f_r), the apparent mass at resonance (AM_r), segmental masses (m_0, m_1 and m_2), stiffnesses (k_1 and k_2) and damping constants (c_1 and c_2) were obtained.

3. Results

3.1. Response in the longitudinal (z-axis) direction

3.1.1. Overview

The individual apparent masses and phases of twelve subjects with five vibration magnitudes of continuous random vibration are shown in Fig. 3. The median normalised apparent masses and phases of the group of 12 subjects are shown in Fig. 4. The medians and ranges of individual apparent mass resonance frequencies are shown in Table 2. The individual apparent masses and phases of the 12 subjects at two vibration magnitudes (0.25 and 1.0 ms^{-2} rms) with both continuous and intermittent random vibration are shown in Fig. 5.

Consistently low target errors (Eq. (4)) were obtained by curve fitting to the two-degree-of-freedom model (Fig. 6). The results of the curve fitting for one subject (Subject 11) are shown for five magnitudes of continuous random vibration in Fig. 7. The fitting results of the vertical in-line apparent mass of the same semi-supine subject were shown in the preceding vertical study [14].

The coherencies were generally in excess of 0.9 in the frequency range 0.5–6.0 Hz. The coherency reduced over a band of higher frequencies, with the frequency of the coherency drop decreasing with increasing vibration magnitude (e.g., 8–20 Hz at 0.125 ms^{-2} rms and 6–18 at 1.0 ms^{-2} rms). The lowest coherency (0.1–0.5) occurred with the highest vibration magnitude (1.0 ms^{-2} rms) in the range 10–16 Hz. The lowest coherency tended to decrease from about 0.5 to about 0.1 as the vibration magnitude increased from 0.125 to 1.0 ms^{-2} rms. The coherencies obtained with intermittent random vibration had a similar pattern to those with continuous random vibration.

There was one dominant resonance frequency in the longitudinal apparent mass between 2.0 and 4.0 Hz. Since the magnitude of the apparent mass at frequencies greater than 5 Hz was small (less than 8% of the apparent mass at resonance), the minor secondary resonance expected at a higher frequency than the primary resonance was not clear. The secondary resonance was expected as it occurs in the apparent mass at the back when subjects seated upright with a backrest are exposed to vertical whole-body vibration, especially at low magnitudes [16]. In the present results, the secondary resonances between about 6 and 10 Hz could be seen with only some subjects (Subjects 2, 8, 9 and 12) and only at very low vibration magnitudes by referring to the phase (Fig. 3).

3.1.2. Apparent mass resonance frequencies with continuous random vibration

The median resonance frequencies of the apparent masses of the 12 subjects decreased from 3.7 to 2.4 Hz as the vibration magnitude increased from 0.125 to 1.0 ms^{-2} rms (Table 2).

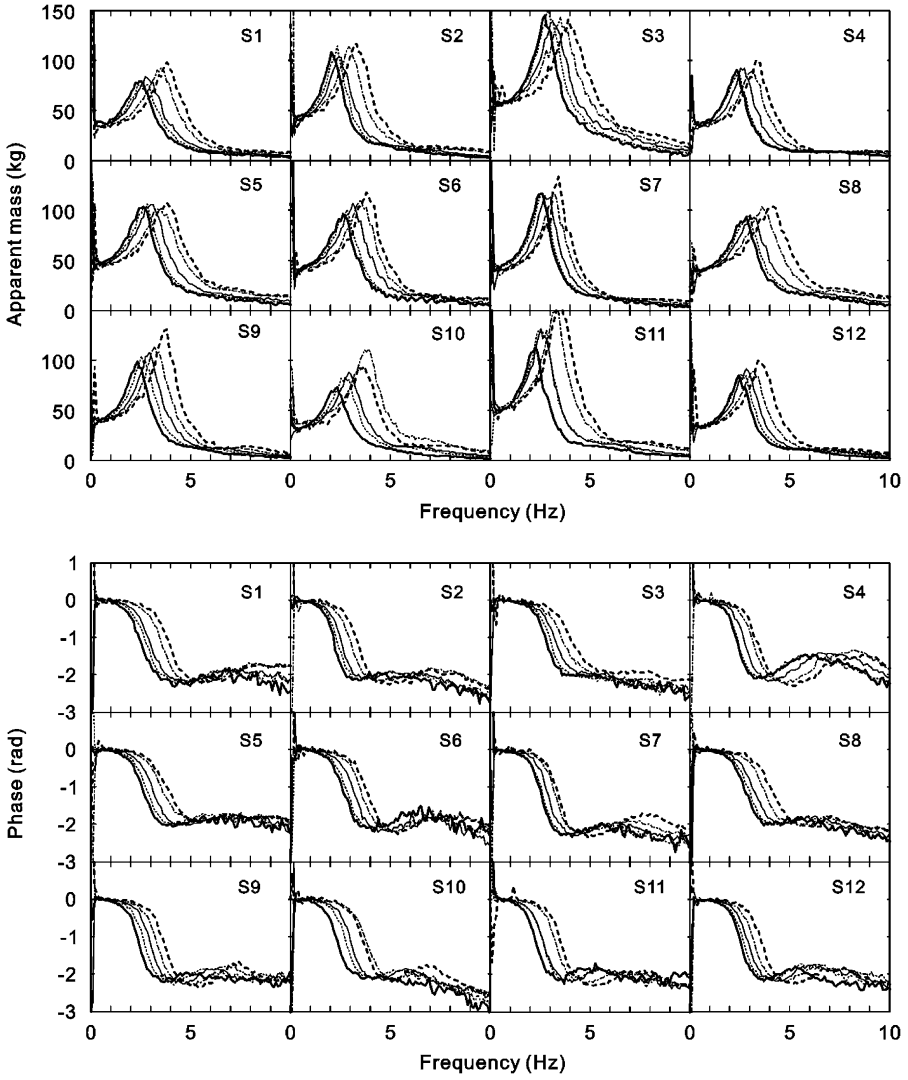

Fig. 3. Individual apparent masses (upper) and phases (lower) of 12 subjects (S1 to S12) at five vibration magnitudes (- - - - - 0.125 ms^{-2} rms; —·—·—·—·— 0.25 ms^{-2} rms; ——— 0.5 ms^{-2} rms; ····· 0.75 ms^{-2} rms; ▬▬ 1.0 ms^{-2} rms) of continuous random vibration.

Over the five vibration magnitudes, the apparent mass resonance frequency (f_r) decreased significantly with increasing magnitude ($p<0.01$, Friedman two-way analysis of variance). There was a significant difference between the resonance frequencies at each of the five magnitudes ($p<0.01$, Wilcoxon matched-pairs signed ranks test).

The resonance frequencies of the median normalised apparent masses (Fig. 4) of the group of 12 subjects were 3.6, 3.3, 2.8, 2.6 and 2.4 Hz with vibration magnitudes of 0.125, 0.25, 0.5, 0.75 and 1.0 ms^{-2} rms, respectively.

3.1.3. Parameters of the two-degree-of-freedom model fitted to the apparent masses with continuous random vibration

The medians and ranges of the parameters of the two-degree-of-freedom model fitted to individual apparent masses and phases are shown in Table 3. The segmental mass m_1, stiffness k_1 and damping constant c_1, determine the primary resonance between 2.0 and 4.0 Hz. The apparent mass at resonance, AM_r (i.e. the

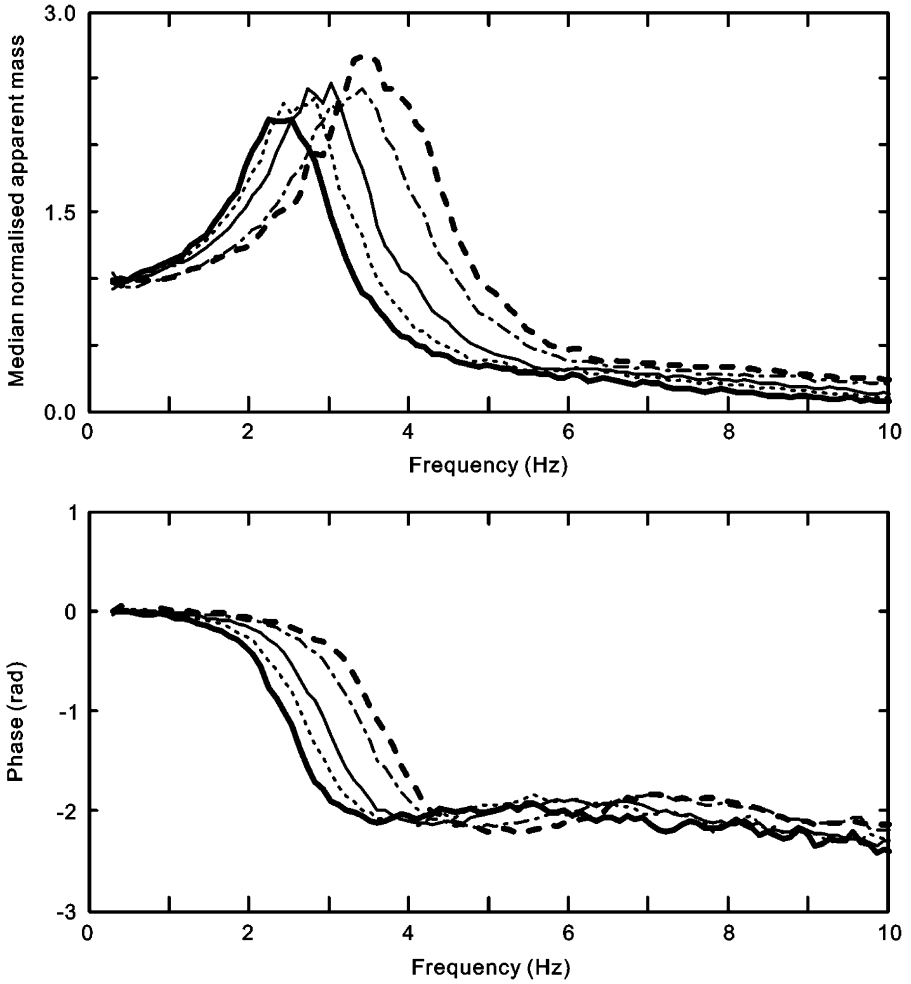

Fig. 4. Median normalised apparent masses (upper) and phases (lower) of the group of 12 subjects at five vibration magnitudes (- - - - - $0.125\,ms^{-2}$ rms; —·—·—·—·— $0.25\,ms^{-2}$ rms; ——— $0.5\,ms^{-2}$ rms; ····· $0.75\,ms^{-2}$ rms; ▬▬ $1.0\,ms^{-2}$ rms) of continuous random vibration.

Table 2
Median and ranges of resonance frequencies of apparent masses generated by fitting the two-degree-of-freedom parametric model to the apparent masses and phases of 12 subjects at five vibration magnitudes (0.125, 0.25, 0.5, 0.75 and $1.0\,ms^{-2}$ rms) of continuous random vibration

Resonance frequency (Hz)	Minimum	Median	Maximum
$f_{0.125}$	3.3	3.7	4.0
$f_{0.25}$	2.9	3.4	3.7
$f_{0.5}$	2.4	2.8	3.2
$f_{0.75}$	2.3	2.6	2.9
$f_{1.0}$	2.2	2.4	2.7

$f_{0.125}$, $f_{0.25}$, $f_{0.5}$, $f_{0.75}$ and $f_{1.0}$: resonance frequencies at five vibration magnitudes (0.125, 0.25, 0.5, 0.75 and $1.0\,ms^{-2}$ rms).

maximum value of the apparent mass modulus of the fitted curve), reflects the damping characteristic of the primary resonance. The segmental mass m_2, stiffness k_2 and damping constant c_2, determine the secondary resonance between 6.0 and 10.0 Hz. The frame mass, m_0, was included improve the fitting [15].

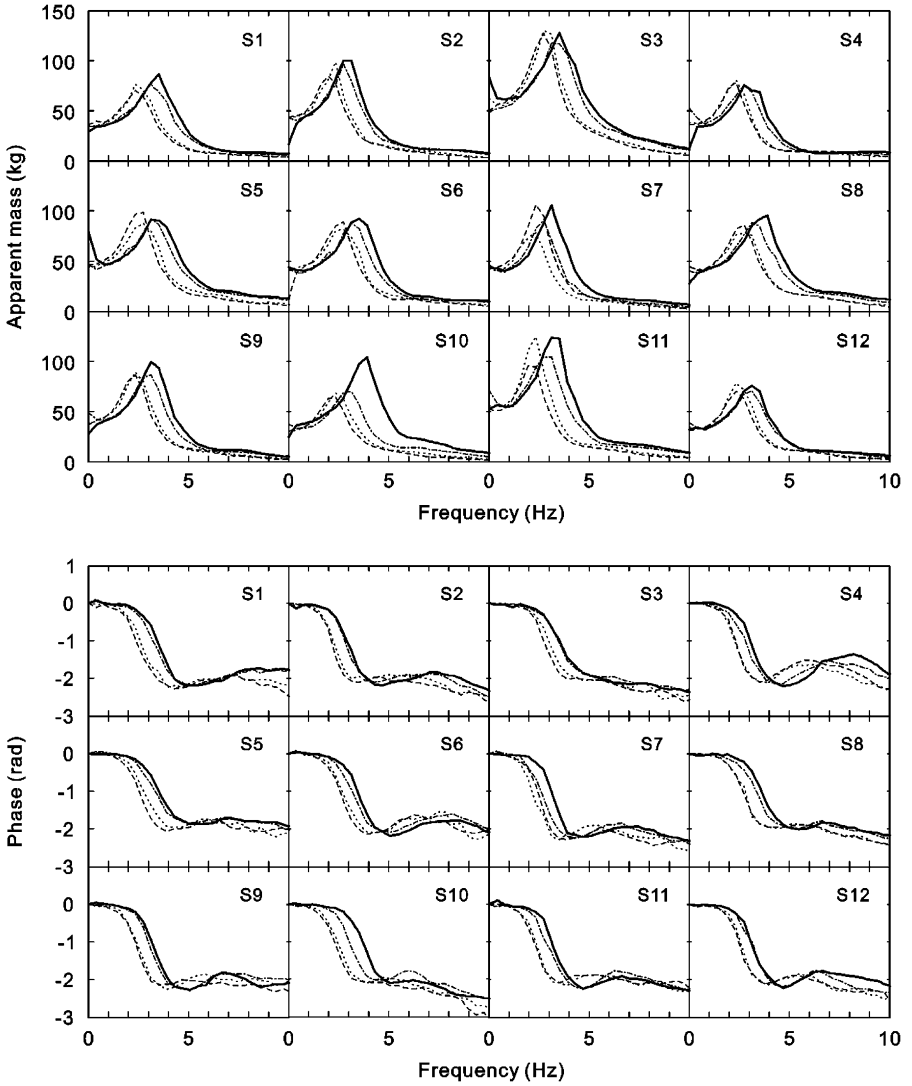

Fig. 5. Individual apparent masses (upper) and phases (lower) of 12 subjects (S1 to S12) at two vibration magnitudes (—·—·—·—·— 0.25 ms^{-2} rms intermittent; ····· 1.0 ms^{-2} rms intermittent; ——— 0.25 ms^{-2} rms continuous; - - - - - 1.0 ms^{-2} rms continuous) of both intermittent random vibration and continuous random vibration.

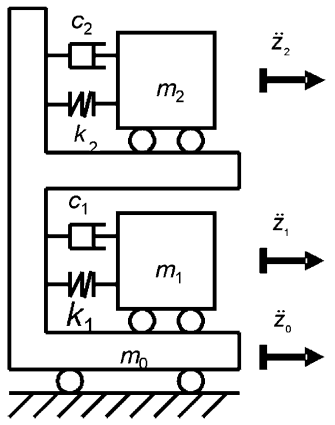

Fig. 6. Parallel two-degree-of-freedom lumped parameter model used to fit longitudinal in-line apparent masses and phases so as to obtain resonance frequencies.

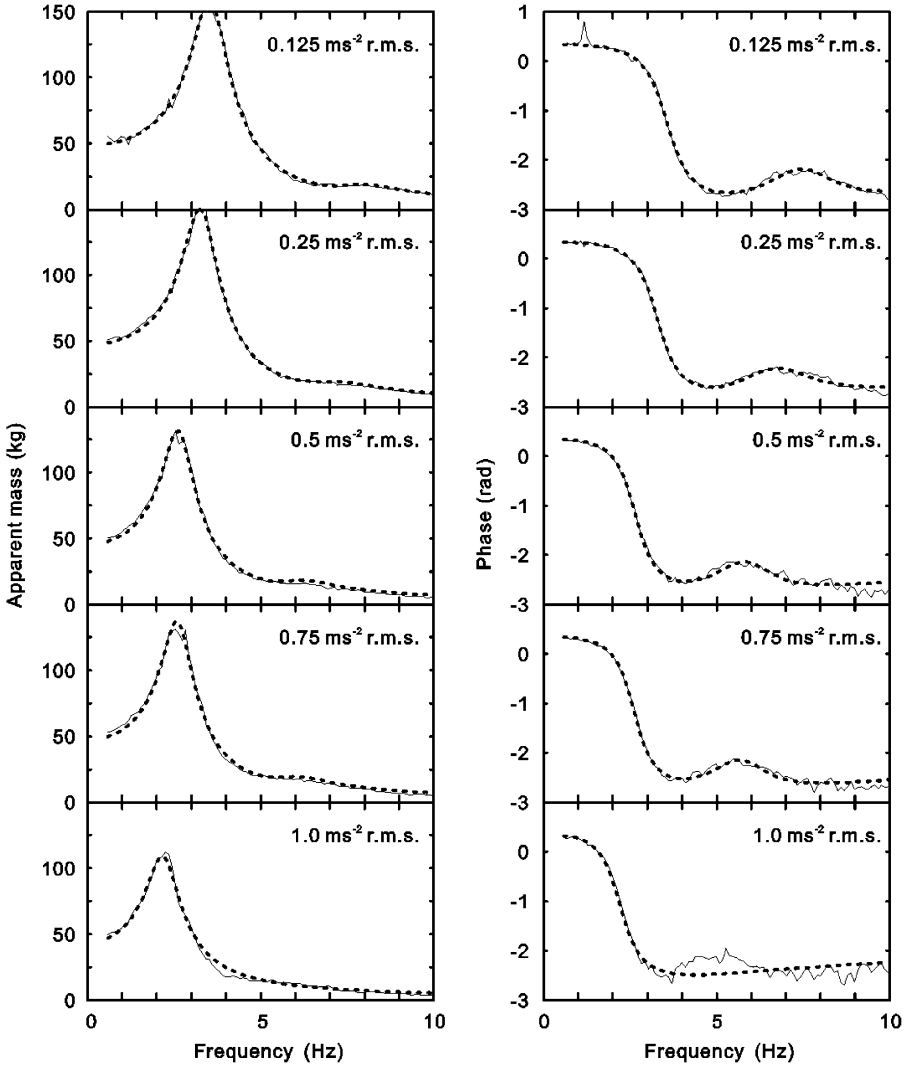

Fig. 7. An example of curve-fitting (——— measurement; - - - - - fitted curve) the apparent masses and phases of one subject (S11) at five magnitudes (0.125, 0.25, 0.5, 0.75, 1.0 ms^{-2} rms) of continuous random vibration to obtain the resonance frequencies. Frequency range of curve fitting: 0.5–10 Hz.

According to the curve fitting, 20 of 60 cases (12 subjects and 5 vibration magnitudes) showed a zero secondary segmental mass (m_2), and most cases exhibited the response of a single-degree-of-freedom system (Fig. 3). Nevertheless, the two-degree-of-freedom model gave a better fit than a single-degree-of-freedom model. The fitting error caused by the phase of the secondary resonance peak was reduced by adding the second-degree-of-freedom in the model (see phases in Fig. 7). The changes in the parameters of the minor secondary resonance (m_2, k_2 and c_2,) at varying magnitudes were not apparent and they are not discussed.

3.1.3.1. The frame mass, m_0. The median value of the frame mass, m_0, decreased from 1.8 to 1.1 kg when the magnitude increased from 0.125 to 0.25 ms^{-2} rms (Table 3). The median m_0 was zero at the three highest magnitudes (0.5, 0.75 and 1.0 ms^{-2} rms). The five vibration magnitudes had a significant overall effect on the frame mass ($p<0.001$, Friedman). The frame mass decreased with increasing magnitude ($p<0.01$, Wilcoxon), except between 0.5 and 0.75 ms^{-2} rms ($p=0.116$, Wilcoxon), between 0.5 and 1.0 ms^{-2} rms ($p=0.075$, Wilcoxon) and between 0.75 and 1.0 ms^{-2} rms ($p=0.066$, Wilcoxon).

Table 3
Median and full ranges of parameters generated by fitting the two-degree-of-freedom parametric model to the apparent masses and phases of 12 subjects at five vibration magnitudes (0.125, 0.25, 0.5, 0.75 and 1.0 ms^{-2} rms) of continuous random vibration

Vibration magnitude (ms^{-2} rms)	m_0 (kg)	m_1 (kg)	k_1 ($N\,m^{-1}$)	c_1 ($Ns\,m^{-1}$)	m_2 (kg)	k_2 ($N\,m^{-1}$)	c_2 ($Ns\,m^{-1}$)	f_r (Hz)	AM_r (kg)
0.125									
Min	0.3	27.4	13429	192	0.9	2777	16	3.3	96.0
Median	1.8	33.0	17743	230	1.9	5037	29	3.7	112.2
Max	3.5	49.1	33581	528	3.7	8651	114	4.0	158.8
0.25									
Min	0.0	27.7	11219	184	0.0	0	8	2.9	90.6
Median	1.1	34.3	16119	259	1.9	3813	34	3.4	109.3
Max	3.3	50.3	27163	475	3.1	7106	105	3.7	150.1
0.5									
Min	0.0	28.5	8699	171	0.0	0	20	2.4	83.0
Median	0.0	35.8	12307	248	1.8	3497	46	2.8	103.4
Max	1.2	49.0	21314	393	2.8	6284	112	3.2	140.7
0.75									
Min	0.0	29.3	6862	165	0.0	0	27	2.3	79.0
Median	0.0	35.5	10296	235	1.1	1408	66	2.6	99.9
Max	0.5	49.6	18211	343	3.0	5701	115	2.9	150.1
1.0									
Min	0.0	25.8	5832	132	0.0	0	26	2.2	80.9
Median	0.0	36.5	8565	217	0.0	0	98	2.4	98.1
Max	0.4	47.4	15288	305	3.1	5732	130	2.7	144.5

m_0, m_1 and m_2—segmental masses. k_1 and k_2—segmental stiffnesses. c_1 and c_2—segmental damping constants. f_r—apparent mass resonance frequency obtained by model. AM_r—apparent mass at resonance by model.

3.1.3.2. The primary segmental mass, m_1. The median value of m_1 increased from 33.0 to 36.5 kg with increasing vibration magnitude from 0.125 to 1.0 ms^{-2} rms except for 0.75 ms^{-2} rms (Table 3). There were small but significant increases in the primary segmental mass with increasing vibration magnitude ($p = 0.017$, Friedman): the primary segmental mass increased with increasing magnitude only between 0.125 and 0.5 ms^{-2} rms ($p = 0.028$, Wilcoxon) and between 0.125 and 0.75 ms^{-2} rms ($p = 0.008$, Wilcoxon).

3.1.3.3. The primary segmental stiffness, k_1. The median value of k_1 decreased from 17743 to 8565 N/m as vibration magnitude increased from 0.125 to 1.0 ms^{-2} rms (Table 3). The vibration magnitude had a significant effect on the primary segmental stiffness ($p < 0.01$, Friedman): the primary segmental stiffness decreased with increasing magnitude ($p < 0.05$, Wilcoxon) with no exception for all five vibration magnitudes.

3.1.3.4. The primary segmental damping constant, c_1. The median value of c_1 decreased from 259 to 217 Ns/m as vibration magnitude increased from 0.25 to 1.0 ms^{-2} rms (Table 3). The vibration magnitude had a small but significant effect on the primary segmental damping constant ($p = 0.005$, Friedman): the primary segmental damping constant decreased with increasing magnitude only between 0.125 and 1.0 ms^{-2} rms ($p = 0.012$, Wilcoxon), between 0.25 and 1.0 ms^{-2} rms ($p = 0.003$, Wilcoxon), and between 0.5 and 1.0 ms^{-2} rms ($p = 0.012$, Wilcoxon).

3.1.3.5. The apparent mass at resonance, AM_r. The median apparent mass at resonance decreased from 112.2 to 98.1 kg as vibration magnitude increased from 0.125 to 1.0 ms^{-2} rms (Table 3). The vibration magnitudes had a significant overall effect on the apparent mass at resonance ($p = 0.002$, Friedman). The apparent mass at resonance decreased with increasing magnitude ($p < 0.05$, Wilcoxon), except between 0.125 and 0.25 ms^{-2} rms ($p = 0.05$, Wilcoxon), between 0.5 and 0.75 ms^{-2} rms ($p = 0.784$, Wilcoxon), between 0.5 and 1.0 ms^{-2} rms ($p = 0.239$, Wilcoxon), and between 0.75 and 1.0 ms^{-2} rms ($p = 0.388$, Wilcoxon).

3.1.4. Apparent mass resonance frequencies with intermittent random vibration

With intermittent random vibration, the median resonance frequency of the apparent mass was 3.0 Hz at 0.25 ms^{-2} rms and 2.4 Hz at 1.0 ms^{-2} rms. Whereas with continuous random vibration, the resonance frequency was 3.3 Hz at 0.25 ms^{-2} rms and 2.4 Hz at 1.0 ms^{-2} rms (Table 4A).

The resonance frequencies with intermittent random vibration at 0.25 ms^{-2} rms were significantly lower than those with continuous random vibration at the same magnitude ($p = 0.003$, Wilcoxon). The effect was apparent for all except Subject 3 (Table 4A and Fig. 5). There was no significant difference in the resonance frequencies with intermittent and continuous vibration at 1.0 ms^{-2} rms ($p = 0.103$, Wilcoxon). However, eight of the twelve subjects (subjects 1, 2, 3, 6, 9, 10, 11 and 12) had higher resonance frequencies with intermittent vibration than with continuous vibration (Table 4A and Fig. 5).

The absolute difference between the resonance frequencies at 0.25 and 1.0 ms^{-2} rms was less with intermittent random vibration than with the continuous random vibration for all 12 subjects ($p = 0.002$, Wilcoxon; Table 4A and Fig. 5).

3.1.5. Parameters of the two-degree-of-freedom model fitted to the apparent masses with intermittent random vibration

The medians and ranges of the parameters of the two-degree-of-freedom model fitted to individual apparent masses and phases are shown in Table 4B.

At 1.0 ms^{-2} rms, the primary segmental stiffness (k_1) was significantly greater ($p = 0.028$, Wilcoxon) with intermittent vibration than with continuous vibration (only subject 7 showed the reverse trend), consistent with the characteristics of thixotropy. At 0.25 ms^{-2} rms, the primary segmental stiffness (k_1) was significantly less ($p = 0.008$, Wilcoxon) with intermittent vibration than with the continuous vibration (only subject 3 showed the reverse trend), also consistent with the thixotropy.

At 1.0 ms^{-2} rms, the primary segmental damping constant (c_1) was significantly greater ($p = 0.038$, Wilcoxon) with intermittent vibration than with continuous vibration (4 subjects showed the reverse trend). However, at 0.25 ms^{-2} rms there was no significant difference in the secondary segmental damping constant (c_1) between the continuous and the intermittent stimulus ($p = 0.456$, Wilcoxon).

At 0.25 ms^{-2} rms, the apparent mass at resonance (AM_r) was significantly less ($p = 0.002$, Wilcoxon) with intermittent vibration than with continuous vibration for all twelve subjects. However, at 1.0 ms^{-2} rms there was no significant difference in the apparent mass at resonance (AM_r) between the continuous and the intermittent stimulus ($p = 0.61$, Wilcoxon).

For the other parameters in the two-degree-of-freedom model, there were no significant differences between the continuous and the intermittent vibration at either 0.25 or 1.0 ms^{-2} rms.

3.2. Response in the vertical (x-axis) cross-axis direction

3.2.1. Overview

The individual vertical (x-axis) cross-axis apparent masses of the 12 subjects with the five magnitudes of continuous random vibration are shown in Fig. 8. The median normalised cross-axis apparent masses of the group of 12 subjects are shown in Fig. 9. The median and ranges of the individual peak frequencies are shown in Table 5. The individual cross-axis apparent masses of the 12 subjects with two vibration magnitudes (0.25 and 1.0 ms^{-2} rms) with both continuous and intermittent random vibration are shown in Fig. 10. The magnitude of the vertical x-axis cross-axis apparent mass at peak were about 60% of the static weight of each subject and were about between 20% and 40% of the magnitude of the horizontal apparent mass at resonance (Fig. 9).

The coherencies were generally in excess of 0.8 at frequencies between 2 and 6 Hz. Some subjects exhibited the lowest coherency (0.1–0.4) at frequencies between 8 and 14 Hz, while some occurred above 18 Hz. Similar to the coherency of the longitudinal in-line apparent mass, there was a drop in the coherency, with the frequency range of the coherency drop decreasing with increasing vibration magnitude. The coherencies with intermittent vibration were of the same pattern as observed with the continuous vibration (Section 3.1.1).

There were two or three distinguishable peaks in each cross-axis apparent mass curve: the number and the magnitude of the peaks varied between subjects and depended on the magnitude of vibration (Fig. 8).

Table 4
Medians and ranges of resonance frequencies (A) and model parameters (B) generated by fitting the two-degree-of-freedom parametric model to the apparent masses and phases of 12 subjects at two vibration magnitudes (0.25 and 1.0 ms^{-2} rms) of both continuous and intermittent random vibration

(*A*) *Resonance frequency* (*Hz*)

Subject	0.25 ms^{-2} rms intermittent	0.25 ms^{-2} rms continuous	1.0 ms^{-2} rms intermittent	1.0 ms^{-2} rms continuous
s1	3.2	3.4	2.5	2.4
s2	2.7	2.9	2.2	2.1
s3	3.4	3.4	2.9	2.7
s4	2.7	3.0	2.3	2.3
s5	3.2	3.4	2.6	2.6
s6	3.1	3.4	2.6	2.5
s7	2.6	3.1	2.2	2.4
s8	3.2	3.6	2.6	2.6
s9	3.0	3.2	2.3	2.3
s10	2.9	3.8	2.3	2.3
s11	2.8	3.2	2.3	2.2
s12	3.0	3.1	2.5	2.4
Minimum	2.6	2.9	2.2	2.1
Median	3.0	3.3	2.4	2.4
Maximum	3.4	3.8	2.9	2.7

(*B*) *Model parameters*

Vibration magnitude (ms^{-2} rms)	m_0 (kg)	m_1 (kg)	k_1 (N m^{-1})	c_1 (Ns m^{-1})	m_2 (kg)	k_2 (N m^{-1})	c_2 (Ns m^{-1})	f_r (Hz)	AM_r (kg)
0.25 Int									
Min	0.0	27.9	9860	229	0.0	0	4	2.6	71.7
Median	0.0	34.2	12725	268	0.0	0	130	3.0	91.4
Max	2.0	50.2	25315	530	5.7	4125	310	3.4	120.4
0.25 Con									
Min	0.0	28.0	11045	207	0.4	0	14	2.9	81.8
Median	0.0	34.2	15995	285	2.4	2339	54	3.3	101.7
Max	1.4	45.8	23015	475	6.9	7106	1487	3.8	131.4
1.0 Int									
Min	0.0	29.7	6915	197	0.0	0	11	2.2	70.6
Median	0.0	36.4	8897	263	0.0	0	128	2.4	88.0
Max	0.7	50.1	18416	417	2.2	3717	183	2.9	129.1
1.0 Con									
Min	0.0	14.8	4430	80	0.0	0	1	2.1	69.5
Median	0.0	36.8	7899	242	0.0	0	158	2.4	91.2
Max	1.0	51.6	16294	427	29.8	6893	282	2.7	126.1

int—intermittent. con—continuous. m_0, m_1 and m_2—segmental masses. k_1 and k_2—segmental stiffnesses. c_1 and c_2—segmental damping constants. f_r—apparent mass resonance frequency of the model. AM_r—apparent mass at resonance by model.

At 0.125 ms^{-2} rms, all twelve subjects showed a dominant primary peak between 3.3 and 4.5 Hz, with some (subjects 1, 2, 4, 5, 7, 8, 11 and 12) showing a secondary peak between 6.0 and 10.0 Hz. At 1.0 ms^{-2} rms, the primary peak frequency was between 2.2 and 3.0 Hz, with no apparent second peak (Figs. 8). The primary peak was used to investigate the effects of magnitude and intermittency on the dynamic characteristic of the cross-axis response (Section 2.5.3).

3.2.2. Vertical (x-axis) cross-axis apparent mass peak frequencies with continuous random vibration

The median peak frequencies of the cross-axis apparent masses of the twelve subjects decreased from 3.8 to 2.5 Hz as the vibration magnitude increased from 0.125 to 1.0 ms^{-2} rms (Table 5A).

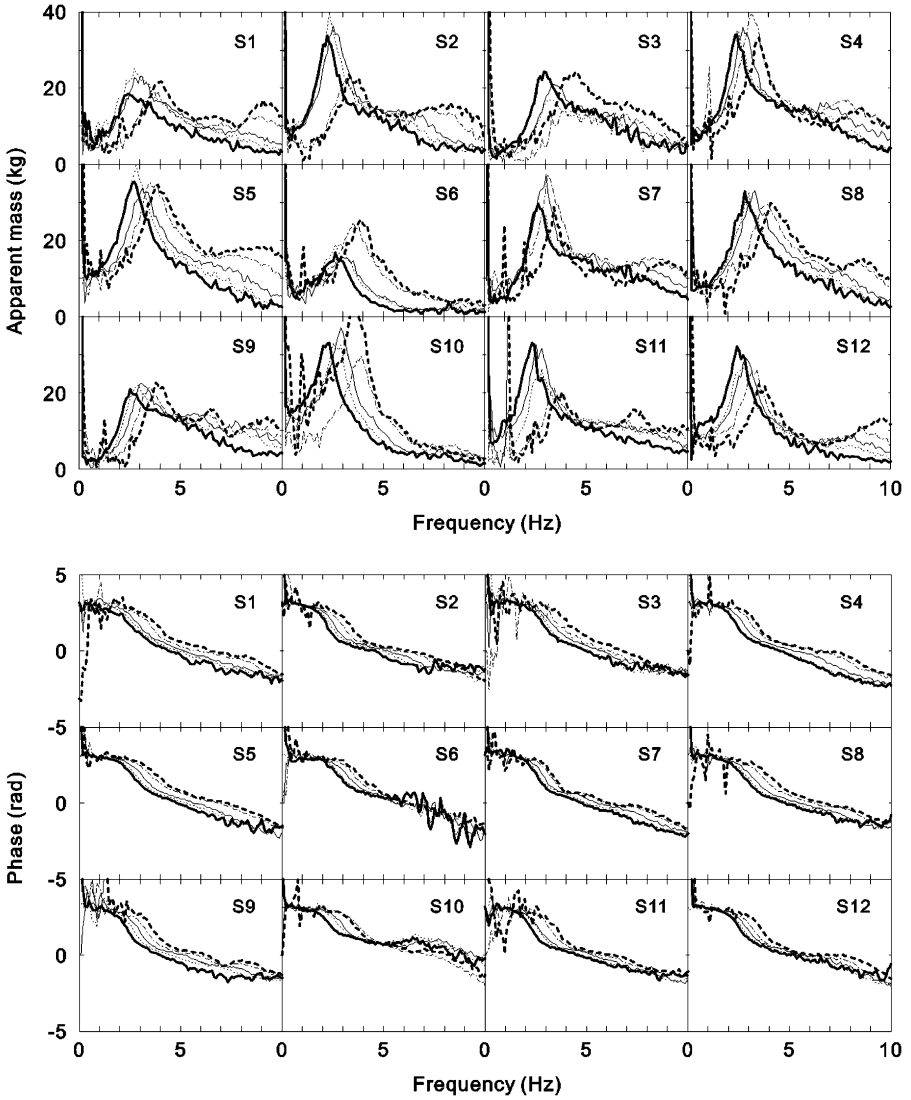

Fig. 8. Individual vertical x-axis cross-axis apparent masses (upper) and phases (lower) of 12 subjects (S1 to S12) at five vibration magnitudes (- - - - - 0.125 ms^{-2} rms; —·—·—·—·— 0.25 ms^{-2} rms; ——— 0.5 ms^{-2} rms; ····· 0.75 ms^{-2} rms; ▬▬ 1.0 ms^{-2} rms) of continuous random vibration.

There was a significant effect of vibration magnitude on the vertical (x-axis) cross-axis apparent mass peak frequencies ($p<0.001$, Friedman). The peak frequency decreased significantly with increasing vibration magnitude from 0.125 to 1.0 ms^{-2} rms ($p<0.02$, Wilcoxon). There was no significant difference in the peak frequencies between 0.75 and 1.0 ms^{-2} rms ($p=0.14$, Wilcoxon). No significant difference was found among the cross-axis apparent masses at peak at the five vibration magnitudes ($p=0.287$, Friedman).

The peak frequencies of the median normalised cross-axis apparent masses of the group of the twelve subjects were 3.8, 3.5, 3.1, 2.7 and 2.3 Hz with vibration magnitudes of 0.125, 0.25, 0.5, 0.75 and 1.0 ms^{-2} rms, respectively (Fig. 9).

There were significant correlations between the cross-axis peak frequencies and the in-line resonance frequencies at 1.0 ms^{-2} rms ($r=0.903$, $p<0.001$, Spearman's rank order correlation test), 0.75 ms^{-2} rms ($r=0.661$, $p=0.019$, Spearman), 0.5 ms^{-2} rms ($r=0.83$, $p=0.001$, Spearman), 0.25 ms^{-2} rms ($r=0.898$, $p<0.001$, Spearman) ms^{-2} rms and 0.125 ms^{-2} rms ($r=0.952$, $p<0.001$, Spearman) ms^{-2} rms. This may

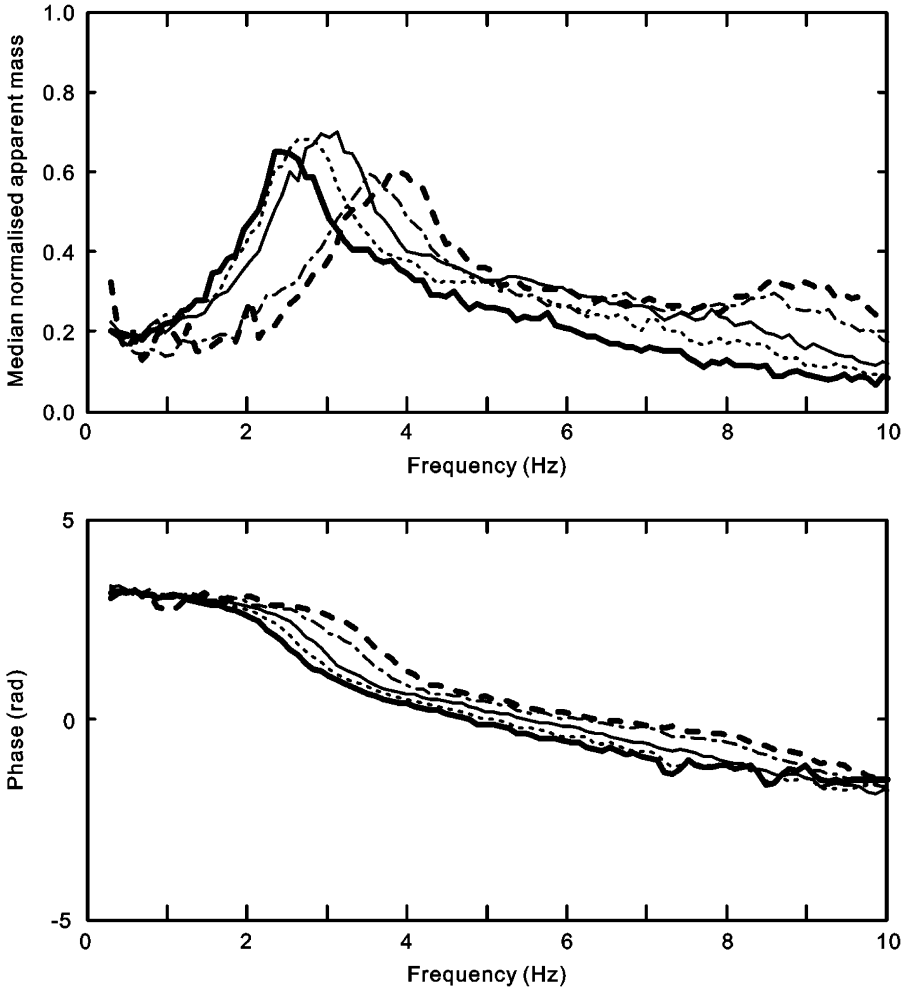

Fig. 9. Median normalised vertical x-axis cross-axis apparent masses (upper) and phases (lower) of the group of 12 subjects at five vibration magnitudes (- - - - - 0.125 ms^{-2} rms; —·—·—·— 0.25 ms^{-2} rms; ——— 0.5 ms^{-2} rms; ····· 0.75 ms^{-2} rms; ▬▬ 1.0 ms^{-2} rms) of continuous random vibration.

imply that the primary resonance occurred in the longitudinal direction and primary peak occurred in the vertical cross-axis direction are correlated to the same mode(s) of the body.

3.2.3. Vertical (x-axis) cross-axis apparent mass peak frequencies with intermittent random vibration

The median peak frequency of the apparent masses with intermittent random vibration was 3.1 Hz at 0.25 ms^{-2} rms and 2.5 Hz at 1.0 ms^{-2} rms. With continuous random vibration, the median peak frequency was 3.5 Hz at 0.25 ms^{-2} rms and 2.7 Hz at 1.0 ms^{-2} rms (Table 5B).

At 0.25 ms^{-2} rms, the peak frequency with intermittent random vibration was significantly lower than the peak frequency with continuous random vibration ($p = 0.002$, Wilcoxon). Only one of the twelve subjects showed the same peak frequencies with the intermittent and the continuous vibration at this magnitude (Table 5B). This implies that the dynamic stiffness of the body in the vertical cross-axis at the low magnitude was lowered by the prior high-magnitude longitudinal vibration. However, at 1.0 ms^{-2} rms, there was no significant difference in the peak frequency with intermittent and continuous vibration ($p = 0.334$, Wilcoxon).

The absolute differences between the peak frequencies with 0.25 and 1.0 ms^{-2} rms were significantly less with the intermittent random vibration than with the continuous random vibration ($p = 0.005$, Wilcoxon). Only subjects 1 and 9 showed marginally reverse trends (Table 5B). The median absolute difference in peak

Table 5
Medians and ranges of peak frequencies of vertical x-axis cross-axis apparent masses of 12 subjects at five vibration magnitudes (0.125, 0.25, 0.5, 0.75 and 1.0 ms^{-2} rms) of continuous random vibration (A), and individual peak frequencies with intermittent and continuous random vibration of 12 subjects at 1.0 and 0.25 ms^{-2} rms (B)

(*A*) *Cross-axis peak frequencies of continuous random vibration* (*Hz*)

Vibration magnitude (ms^{-2} rms)	Minimum	Median	Maximum
0.125	3.3	3.8	4.5
0.25	3.1	3.5	4.3
0.5	2.5	3.0	3.3
0.75	2.3	2.8	3.2
1.0	2.3	2.5	2.9

(*B*) *Cross-axis peak frequencies of intermittent random vibration* (*Hz*)

Subject	0.25 ms^{-2} rms. intermittent	0.25 ms^{-2} rms continuous	1.0 ms^{-2} rms intermittent	1.0 ms^{-2} rms continuous
s1	3.1	3.5	2.3	2.7
s2	3.1	3.2	2.3	2.3
s3	3.9	4.3	3.1	3.1
s4	3.1	3.5	2.7	2.3
s5	3.5	3.9	3.1	2.7
s6	3.1	3.5	2.7	2.7
s7	2.7	3.1	2.3	2.7
s8	3.5	3.9	3.1	2.7
s9	3.5	3.5	2.7	2.7
s10	3.1	3.9	2.3	2.3
s11	3.1	3.5	2.3	2.3
s12	3.1	3.5	2.3	2.3
Minimum	2.7	3.1	2.3	2.3
Median	3.1	3.5	2.5	2.7
Maximum	3.9	4.3	3.1	3.1

frequency between at 1.0 and 0.25 ms^{-2} rms was considerably less with intermittent random vibration (0.8 Hz) than with continuous random vibration (1.2 Hz).

At either the low magnitude or the high magnitude of vibration, the intermittency had no effect on the cross-axis apparent mass at peak (at 1.0 ms^{-2} rms, $p = 0.373$, Wilcoxon; at 0.25 ms^{-2} rms, $p = 1.0$, Wilcoxon).

4. Discussion

4.1. Effect of vibration magnitude on apparent mass resonance frequency and cross-axis apparent mass peak frequency

4.1.1. Response in the longitudinal (z-axis) direction

The longitudinal in-line apparent masses at five magnitudes show that the semi-supine body is nonlinear: the resonance frequencies decreased significantly with increasing vibration magnitude. This is apparent in the primary stiffness, k_1, of the parametric two-degree-of-freedom-model (Section 3.1.3 and Table 3). The characteristic nonlinearity found here is consistent with the nonlinearity in the vertical in-line apparent masses of the same semi-supine subjects during vertical excitation [14]. With both longitudinal horizontal and vertical excitation, the relaxed semi-supine posture is assumed to require no voluntary muscular postural control and minimal involuntary reflex responses for postural control compared to sitting and standing postures. The consistent nonlinear response suggests that the nonlinearity is not primarily caused by voluntary control of postural muscles, but the result of some passive property of the body (e.g. thixotropy) or, alternatively, an involuntary reflex response of the body.

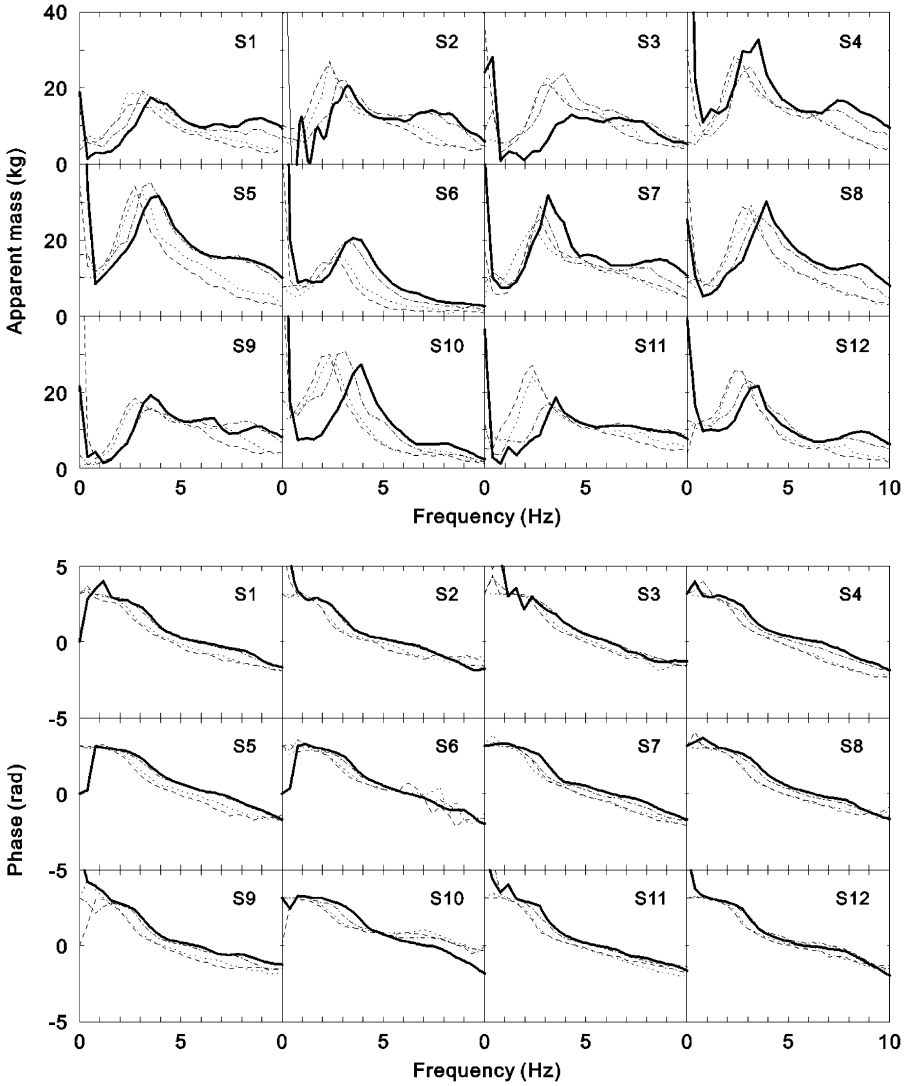

Fig. 10. Individual vertical x-axis cross-axis apparent masses (upper) and phases (lower) of 12 subjects (S1 to S12) at two vibration magnitudes (—·—·—·—·— 0.25 ms^{-2} rms intermittent; ····· 1.0 ms^{-2} rms intermittent; ——— 0.25 ms^{-2} rms continuous; - - - - - 1.0 ms^{-2} rms continuous) of both intermittent random vibration and continuous random vibration.

For subjects sitting upright with minimum thigh contact during vertical whole-body vibration, the vertical apparent mass resonance frequency at the backrest reduced from 7 to 5 Hz as the vibration magnitude increased from 0.125 to 1.25 ms^{-2} rms [16]. The semi-supine posture in the present study showed a considerably lower resonance frequency—the resonance frequency of the median normalised longitudinal in-line apparent mass changed from 3.6 to 2.4 Hz as the magnitude increased from 0.125 to 1.0 ms^{-2} rms. The absence of the seat surface perpendicular to the longitudinal direction (z-axis) of the body in the present semi-supine condition allows more body movement in the longitudinal direction. The movement of semi-supine body might involve shear in the tissues between the supine support surface and the skeletal structure, or within other tissues inside the body.

4.1.2. Response in the vertical (x-axis) cross-axis direction

The vertical x-axis cross-axis apparent masses at the five magnitudes show that the semi-supine body is nonlinear: the peak frequency decreased with increasing vibration magnitude (Table 5A).

The peak frequencies of the vertical x-axis cross-axis apparent masses were correlated with the resonance frequencies of the longitudinal z-axis in-line apparent masses at all five vibration magnitudes (Section 3.2.2). This implies that the responses in the two axes are cross-coupled by some common mechanism. The consistent nonlinear responses in both the longitudinal and the vertical cross axes suggest the nonlinearities in these two directions may have a common cause.

Correlations between the in-line and cross-axis resonance frequencies are also found in the apparent mass and cross-axis apparent mass at the backs of upright sitting subjects during vertical excitation. Nawayseh and Griffin [16] measured the apparent mass and fore-and-aft cross-axis apparent mass on a vertical backrest with upright sitting subjects. The dominant fore-and-aft (x-axis) cross-axis apparent mass peak frequency at the back during vertical (z-axis) whole-body vibration varied over the range 5–10 Hz when the vibration magnitude varied from 1.25 to 0.125 ms^{-2} rms. This is similar to the resonance frequency in the vertical in-line direction at the back while seated (i.e., 5–7 Hz), and similar to the peak in the fore-and-aft and pitch transmissibilities to the spine (T1, T5, T10 and L1) and the pelvis during vertical vibration [17].

In the present study with longitudinal excitation of the semi-supine body, there were large responses in the vertical cross-axis direction: the maximum of the median normalised cross-axis apparent mass (0.6–0.7) was about 26% of the median normalised longitudinal in-line apparent mass at resonance (2.2–2.7). This was not the case with vertical excitation of the semi-supine body [14]: the maximum median normalised longitudinal cross-axis apparent mass (about 0.1) was only about 7% of the maximum median normalised vertical in-line apparent mass (about 1.5).

With subject sitting upright while exposed to vertical excitation, the median fore-and-aft cross-axis apparent mass at the backrest was a maximum of about 25 kg, while the median vertical in-line apparent mass at the backrest was a maximum of about 5 kg [16]. With the same sitting conditions and the same subjects but with fore-and-aft excitation, Nawayseh and Griffin [18] found that the vertical cross-axis apparent mass of one subject at the back was less than 3 kg at all frequencies, while the fore-and-aft in-line apparent mass at the back was between about 60 and 100 kg at resonance, depending on the subject and the vibration magnitude. With subjects either sitting upright or semi-supine, comparing z-axis and x-axis excitation, the cross-axis response in the x-axis is always larger than the cross-axis response in the z-axis. It seems that the cross-coupling mechanism in the human body is stronger for excitations in the z-axis of the body.

4.2. Effect of intermittency on apparent mass resonance frequency and cross-axis apparent mass peak frequency

4.2.1. Response in the longitudinal (z-axis) direction

The results with intermittent vibration appear characteristic of thixotropic changes in the dynamic stiffness of the body: the resonance frequency at a low magnitude (0.25 ms^{-2} rms) was lower with intermittent vibration than with the continuous vibration. The resonance frequency at the low magnitude reflected the dynamic stiffness of the body 2.56 s after high-magnitude 'perturbation'.

With vertical excitation of the semi-supine body [14], the median resonance frequency at 0.25 ms^{-2} rms was 9.3 Hz with intermittent vibration and 9.6 Hz with continuous vibration. So the relative percentage change due to intermittency was 3.5% (i.e. (9.62–9.28)/9.62). In the present study, the relative percentage change was 8.7% (i.e. (3.03–3.32)/3.32, Table 4A), $2\frac{1}{2}$ times greater than with vertical excitation. So the effect of intermittency tended to be greater in the present study with horizontal longitudinal excitation.

It was hypothesised that the resonance frequency at the high magnitude (1.0 ms^{-2} rms) would be higher with intermittent vibration than with continuous vibration, because the resonance frequency at the high magnitude would reflect the dynamic stiffness of the body 2.56 s after the low-magnitude 'stillness'. The difference was not statistically significant, but eight subjects (1, 2, 3, 6, 9, 10, 11, and 12) of the twelve subjects showed this effect at 1.0 ms^{-2} rms (Fig. 5 and Table 4A). Huang and Griffin [10] found that voluntary periodic muscular activity was less effective in changing the resonance frequency at high magnitudes, consistent with voluntary movement having less effect on thixotropy at high magnitudes. At greater magnitudes of vibration there are greater inertial forces that may be sufficient to change thixotropy quickly, so voluntary muscle activity was not needed to reduce the dynamic stiffness of the body. This may explain why intermittency did not significantly alter the stiffness of the body at high magnitudes of vibration. It may be assumed that the dynamic stiffness of the body cannot continue to decrease with ever-increasing vibration magnitude—there must be a limitation for

the body to be able to withstand high-magnitude inertial forces without collapsing. This will limit the maximum reduction in stiffness with high magnitudes and may be expected to differ for different people.

Intermittency had a significant effect on the primary segmental mass (k_1) of the parametric model at both 0.25 and 1.0 ms^{-2} rms and the primary damping constant (c_1) at 1.0 ms^{-2} rms (Section 3.1.5 and Table 4B). Using a similar parametric model, Huang and Griffin [14] found that the effect of intermittency was only significant in k_1 and only at 1.0 ms^{-2} rms for the semi-supine body exposed to vertical excitation. So the effect of intermittency was apparent in more parameters during longitudinal excitation than during vertical excitation.

4.2.2. Response in the vertical (x-axis) cross-axis direction

Similar to the responses in the longitudinal in-line direction, the effect of intermittency was found in the vertical cross-axis direction with 0.25 ms^{-2} rms but not with 1.0 ms^{-2} rms excitation. Since the frequency resolution of the apparent mass during intermittent vibration was originally 0.4 Hz and then linearly interpolated to 0.1 Hz, the small changes in the cross-axis peak frequencies may be masked by the 0.4 Hz resolution. However, this was not the case in the in-line responses as the in-line apparent mass was fitted by the parametric model with 0.1 Hz resolution.

4.3. Effect of vibration magnitude on apparent mass coherency

The frequency band of the reduction in coherency (over the range 6–20 Hz) showed a similar pattern to the nonlinearity in the apparent mass resonance frequency (over the range 2–4 Hz): the frequency band of the coherency drop decreased with increasing vibration magnitude (Fig. 11c). And the lowest coherency decreased with increasing vibration magnitude.

The CSD method of calculating the apparent mass used here assumes that the output force is linearly correlated with the input acceleration. The apparent mass might alternatively be calculated using the PSD method that includes noise and distortion that are not correlated between the input and the output. For measurements from a typical subject, Fig. 11a shows that at all five magnitudes the CSD and the PSD method give similar absolute apparent masses at all frequencies between 0 and 20 Hz. Fig. 11b shows the absolute difference between the apparent mass estimated using the CSD and PSD methods at each of the five magnitudes. This difference is the total 'noise' or distortion between the input acceleration and the output dynamic force. The peak 'noise' occurs over the frequency range of the apparent mass resonance (2–4 Hz), so the absolute 'noise' is proportionally greater with greater body movement. At frequencies greater than 6 Hz, the output force is much less and, as a consequence, the 'noise' has a relatively greater effect on the coherency, as shown in Fig. 11c. The noise-output ratio (the absolute difference between the apparent mass modulus obtained by the PSD method and the apparent mass modulus obtained by the CSD method divided by the apparent mass modulus obtained using the CSD method) is shown in Fig. 11d. The frequency with the greatest noise-output ratio decreases with increasing vibration magnitude and the ratio at the peak frequency tends to be greater with greater magnitudes of vibration. These changes around 10–16 Hz (as seen in Fig. 11c and d) probably occur because the nonlinearity results in reductions in the output force at high frequencies rather than because there is greater 'noise' at these frequencies. The same trends were observed for all twelve subjects.

Previous studies with standing, sitting, and semi-supine postures during vertical excitation have not reported systematic drops in coherency. Normally, coherency drops with low-magnitude excitation (e.g. 0.125–0.25 ms^{-2} rms) and at low frequencies (e.g. less than 1–2 Hz) due to small input signals and noise at the output (e.g. subject voluntary or involuntary movement). In the present study with longitudinal horizontal excitation, subjects reported more overall movement and more local movement (e.g. from body components within the trunk and hip) along the direction of excitation than during vertical (x-axis) excitation [14].

5. Conclusions

With continuous random longitudinal excitation, the longitudinal in-line apparent mass resonance frequencies and vertical cross-axis apparent mass peak frequencies of the relaxed semi-supine human body decrease with increasing vibration magnitude from 0.125 to 1.0 ms^{-2} rms.

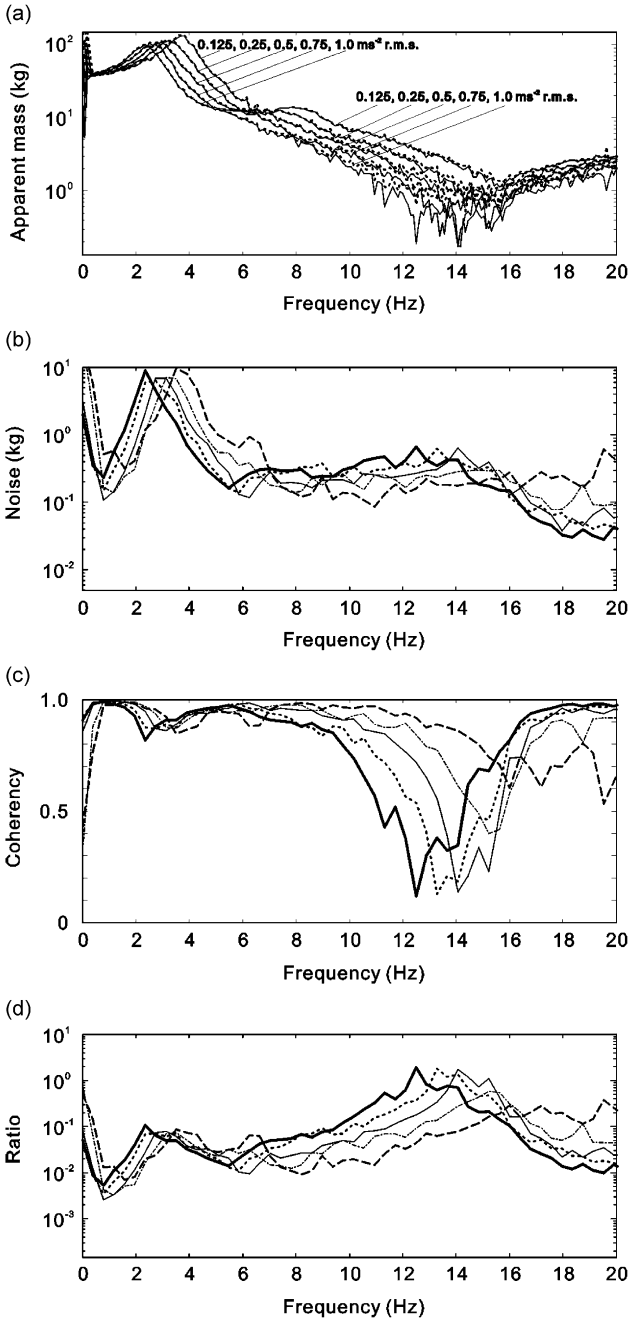

Fig. 11. Comparison of the PSD and the CSD method for one individual subject (S9) with a frequency resolution 0.4 Hz. (a) Apparent mass modulus using the CSD (————) and the PSD (- - - - -) method at five magnitudes of vibration (0.125, 0.25, 0.5, 0.75, 1.0 ms^{-2} rms). (b) Noise—absolute difference between the apparent mass modulus using the PSD method and the CSD method at five vibration magnitudes (▬ ▬ ▬ 0.125 ms^{-2} rms; —·—·—·— 0.25 ms^{-2} rms; ——— 0.5 ms^{-2} rms; - - - - - 0.75 ms^{-2} rms; ▬▬▬ 1.0 ms^{-2} rms). (c) Coherencies at five magnitudes of vibration; (d) Ratio of the absolute noise (see (b)) over the apparent mass modulus using the CSD method at five vibration magnitudes with continuous random vibration.

With intermittent excitation, the in-line resonance frequency and the cross-axis peak frequency measured at a low magnitude (0.25 ms^{-2} rms) decreased immediately after prior exposure to a higher magnitude of vibration (1.0 ms^{-2} rms), compared to the resonance frequency and peak frequency measured at 0.25 ms^{-2} rms

with continuous vibration. With intermittent vibration, the in-line resonance frequency and the cross-axis peak frequency were similar at a high magnitude ($1.0\,ms^{-2}$ rms) to that measured with continuous vibration.

It is concluded that the passive thixotropic behaviour of the human body is likely to be at least partially responsible for reduced resonance frequencies with higher vibration magnitudes—as the vibration magnitude increases, the movement of tissues reduces their overall stiffness. However, reflex muscle activity may also have an influence.

References

[1] N.J. Mansfield, M.J. Griffin, Non-linearities in apparent mass and transmissibility during exposure to whole-body vertical vibration, *Journal of Biomechanics* 33 (2000) 933–941.
[2] N.J. Mansfield, M.J. Griffin, Effects of posture and vibration magnitude on apparent mass and pelvis rotation during exposure to whole-body vertical vibration, *Journal of Sound and Vibration* 253 (1) (2002) 93–107.
[3] N. Nawayseh, M.J. Griffin, Non-linear dual-axis biodynamic response to vertical whole-body vibration, *Journal of Sound and Vibration* 268 (2003) 503–523.
[4] N. Nawayseh, M.J. Griffin, Non-linear dual-axis biodynamic response to fore-and-aft whole-body vibration, *Journal of Sound and Vibration* 282 (2005) 831–862.
[5] Y. Matsumoto, M.J. Griffin, Dynamic response of the standing human body exposed to vertical vibration: influence of posture and vibration magnitude, *Journal of Sound and Vibration* 212 (1) (1998) 85–107.
[6] G.H.M.J. Subashi, Y. Matsumoto, M.J. Griffin, Apparent mass and cross-axis apparent mass of standing subjects during exposure to vertical whole-body vibration, *Journal of Sound and Vibration* 293 (1–2) (2006) 78–95.
[7] P. Holmlund, R. Lundström, Mechanical impedance of the sitting human body in single-axis compared to multi-axis whole-body vibration exposure, *Clinical Biomechanics* 16 (Suppl. 1) (2001) S101–S110.
[8] C.D. Robertson, M.J. Griffin, Laboratory studies of the electromyographic response to whole-body vibration, ISVR Technical Report 184, University of Southampton, 1989.
[9] R. Blüthner, H. Seidel, B. Hinz, Myoelectric response of back muscles to vertical random whole-body vibration with different magnitudes at different postures, *Journal of Sound and Vibration* 253 (1) (2002) 37–56.
[10] Y. Huang, M.J. Griffin, Effect of voluntary periodic muscular activity on nonlinearity in the apparent mass of the seated human body during vertical random whole-body vibration, *Journal of Sound and Vibration* 298 (2006) 824–840.
[11] R.I. Tanner, *Engineering Rheology, Oxford Engineering Science Series 14*, Clarendon Press, Oxford, 1985.
[12] Y.C. Fung, *Biomechanics– Mechanical Properties of Living Tissues*, Springer, New York, 1981.
[13] M. Lakie, Vibration causes stiffness changes (thixotropic behaviour) in relaxed human muscle, United Kingdom Group Informal Meeting on Human Response to Vibration, Loughborough University of Technology, 22–23 September 1986.
[14] Y. Huang, M.J. Griffin, Nonlinear dual-axis biodynamic response of the semi-supine human body during vertical whole-body vibration, *Journal of Sound and Vibration*, in press, doi:10.1016/j.jsv.2007.10.046.
[15] L. Wei, M.J. Griffin, Mathematical models for the apparent mass of the seated human body exposed to vertical vibration, *Journal of Sound and Vibration* 212 (5) (1998) 855–874.
[16] N. Nawayseh, M.J. Griffin, Tri-axial forces at the seat and backrest during whole-body vertical vibration, *Journal of Sound and Vibration* 277 (2004) 309–326.
[17] Y. Matsumoto, M.J. Griffin, Non-linear characteristics in the dynamic responses of seated subjects exposed to vertical whole-body vibration, *Journal of Biomechanical Engineering* 124 (2002) 527–532.
[18] N. Nawayseh, M.J. Griffin, Tri-axial forces at the seat and backrest during whole-body fore-and-aft vibration, *Journal of Sound and Vibration* 281 (2005) 921–942.